Turkish Journal of Electrical Engineering & Computer Sciences

http://journals.tubitak.gov.tr/elektrik/

Research Article

Turk J Elec Eng & Comp Sci
(2019) 27: 634 – 648

doi:10.3906/elk-1805-183

A coordinated DC voltage control strategy for cascaded solid state transformer with star configuration

Zhendong JI[1,*], **Yichao SUN**[2], **Cheng JIN**[2], **Jianhua WANG**[2], **Jianfeng ZHAO**[2]
[1]School of Automation, Nanjing University of Science and Technology, Nanjing, P.R. China
[2]Jiangsu Provincial Key Laboratory of Smart Grid Technology and Equipment, Southeast University, Nanjing, P.R. China

Received: 29.05.2018 • **Accepted/Published Online:** 31.10.2018 • **Final Version:** 22.01.2019

Abstract: Cascaded solid-state transformer (SST) can be directly connected to the high-voltage distribution grid, and it has broad applications in the future smart grid, traction locomotive, and renewable energy integration. However, the reliability of the cascaded SST is seriously influenced by the DC voltage and power imbalance issues with this configuration. This paper presents a coordinated DC voltage control strategy for cascaded SST with star configuration, in which the average DC voltage and the balancing DC voltage are controlled separately without current sensors in dual active bridge (DAB) modules. This strategy not only reduces the cost and the complexity of the control system but also realizes the unbalanced reactive compensation to some extent. Simulation and experimental results verify the feasibility and validity of the proposed method.

Key words: Star configuration, cascaded solid state transformer, dual active bridge, DC voltage balancing, imbalance reactive compensation

1. Introduction

Solid-state transformer (SST) transfers electrical energy via electronic power conversion and electromagnetic coupling of medium/high frequency. Besides the functions of electrical isolation and voltage conversion of traditional power transformer, SST also has abilities of DC output, power quality management, self-protection, interaction with power grid and so on. SST will be one of the key infrastructures in the construction of future energy internet [1, 2].

Many different topologies are proposed in the development of SST, and the type of three-stage topology (AC/DC-DC/AC) is widely adopted nowadays. Although this topology has more switching devices, the DC buses in both the input and output sides improve the control flexibility of electric energy and broaden the scope of application. FREEDM [3] (future renewable electric energy delivery and management) of North Carolina State University, PETT [4] (power electronic traction transformer) of ABB, and IUT [5] (intelligent universal transformer) of EPRI are all researched based on the cascaded SST with three-stage topology, which can be connected to high-voltage distribution grid without using transformer and has become a research hotspot of high-voltage high-power fields in recent years. Compared with delta configuration, the cascaded SST with star configuration reduces both cost and complexity, and is much more suitable for the three-phase system [6, 7]. There are multiple H-bridge modules in series and multiple dual active bridge (DAB) modules in parallel in the cascaded SST. On the one hand, the differences of parameters, losses, pulse delays among H-bridge modules and

*Correspondence: zhendong_ji@126.com

the voltage imbalance of the grid induces DC voltage imbalance problems, which affects the reliable operation of SST [8]. On the other hand, the bias in loss, transformer ratio, and the leakage reactance among DAB modules give rise to imbalanced current distribution, which further leads to uneven heat dissipation and overload currents of some modules under rated load [9]. Therefore, DC voltage and power balance control is the crucial part of the control strategy for the cascaded SST.

DC voltage balancing of cascaded H-bridges can be solved by either the hardware or software method. An additional circuit is needed in the hardware method [10, 11], which increases the cost and the complexity of control. In contrast, the software method, which includes inphase and interphase DC voltage balancing control methods, is more practical. The inphase DC voltage balancing can be solved by adjusting the amplitude or phase angle of each H-bridge voltage modulation wave [12, 13]. Ye et al. [14] applied the idea of inphase to the interphase DC voltage balancing, which is equivalent to control the three phases separately without considering the coupling relationship among three phases. So the regulation range and dynamic performance of the imbalance are limited by this method. Lu et al. [15] proposed a zero-sequence voltage-based interphase voltage balancing method for STATCOM. However, this method has not taken into account the unbalanced factors in the grid side and its regulation ability is relatively weak [15–17], so it is limited in the cascaded SST. In [18], the method of injecting negative-sequence current was proposed for the cascaded H-bridge STATCOM, which can effectively adjust the interphase imbalance with large difference. However, the pollution of power grid caused by the negative-sequence current injection affects the compensation performance of STATCOM.

In most of the previous research [19–24], DC voltage balancing of cascaded H-bridges system and power/current sharing of paralleled DAB modules system are controlled separately to balance DC voltage and DAB module power, which is called independent control for each stage in this paper. In [10–12], different inphase DC balance control methods are proposed for single-phase cascaded H-bridges, while current/power sharing strategy is used for paralleled DAB modules with additional current sensors. Wang et al. [14] proposed a zero-sequence compensation strategy based on three-phase dq decoupled current controller for cascaded SST with star configuration. She et al. [15] proposed a current sensorless power balance control method for single-phase SST, in which current sharing of paralleled DAB modules is adjusted by the intermediate quantity of inphase DC voltage balance control for cascaded H-bridges. However, this method can be hardly extended to three-phase SST with added interphase DC voltage balance control. SST with STATCOM function plays an important role in improving transmission capacity, voltage stability and power quality of power grid [1]. SST not only compensates positive-sequence reactive current, but also compensates negative-sequence current for unbalanced load or system voltage. The existing method only has weak unbalanced reactive power compensation capability [7].

In this paper, a coordinated DC voltage control strategy is proposed for cascaded SST with star configuration. The average DC voltage and reactive power compensation currents are regulated by three-phase dq decoupled current controller, while DC voltage balancing can be achieved by adjustive phase-shifted angles for DAB modules. In the proposed DC voltage balance control method, it is unnecessary to measure currents of DAB modules, which reduces the costs and the complexity of the control system. Moreover, arbitrary imbalance reactive compensation can be realized.

This paper is organized as follows. In Section 2, an average math model of the three-phase cascaded SST is established and the power characteristics are analyzed. Section 3 proposes the coordinated DC voltage control strategy for cascaded SST with star configuration. Simulation and experiment are described respectively in Sections 4 and 5 to validate the effectiveness of the proposed method. Finally, Section 6 presents the conclusions.

2. Power characteristics analysis of cascaded SST

Figures 1a and 1b show the topology of the three-phase cascaded SST with star configuration. This topology consists of cascaded H-bridges and paralleled DAB modules, which correspond to AC-Stage and DC-Stage. DC-AC inverter of the output stage is not studied in this paper.

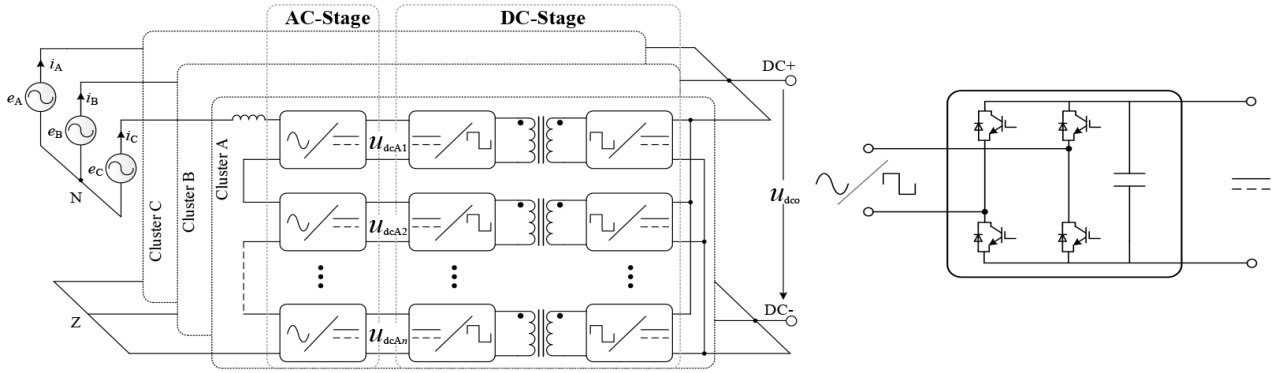

(a) overall structure diagram

(b) unit topology

Figure 1. Topology of cascaded SST.

2.1. Inphase power characteristics

Figure 2 describes the average mathematical model of a single-phase cascaded SST, which is established according to [11–13]. All variables in Figure 2 are average values in a switching period.

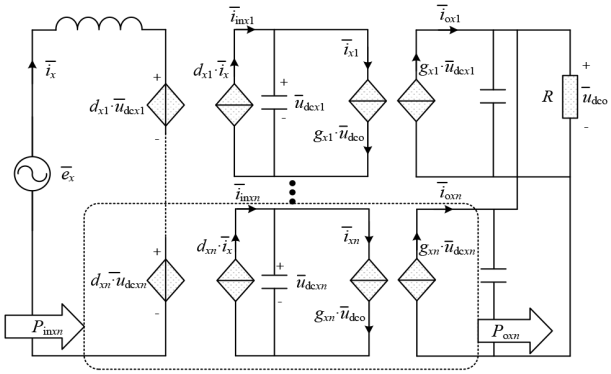

Figure 2. Average mathematical model of single-phase cascaded SST.

Here, x is the phase sequence, e_x is the grid voltage of the phase-x, i_x is the grid-connected current of the phase-x, d_{xn} is the duty cycle of No. n H-bridge in the phase-x, u_{dcxn} is the DC voltage of No. n module in the phase-x, and u_{dcxo} is the output DC voltage of the SST. g_{xn} is the transfer conductance of No. n DAB module in the phase-x, and can be expressed as:

$$g_{xn} = \frac{m_{xn}\varphi_{xn}\left(1-\varphi_{xn}\right)}{2f_{DAB}L_{kxn}}, \tag{1}$$

where m_{xn} is the ratio of medium-frequency transformer, L_{kxn} is the leakage reactance of medium-frequency transformer, i_s the phase-shifted angle, f_{DAB} is the working frequency of switching devices in DAB module.

As shown in Figure 2, under ideal steady-state conditions $d_{x1} = d_{xx} = ... = d_{xn}$, we have $\bar{i}_{inx1} = \bar{i}_{inx2} = ... = \bar{i}_{inxn}$,

$$g_{x1} = g_{x2} = ... = g_{xn}. \tag{2}$$

If $\bar{u}_{dcx1} = \bar{u}_{dcx2} = ... = \bar{u}_{dcxn}$, we will have $\bar{i}_{ox1} = \bar{i}_{ox2} = ... = i\bar{u}_{oxn}$, or if $\bar{i}_{ox1} = \bar{i}_{ox2} = ... = i\bar{u}_{oxn}$, we will have $\bar{u}_{dcx1} = \bar{u}_{dcx2} = ... = \bar{u}_{dcxn}$. So, we conclude that DC voltage balancing of cascaded H-bridges is achieved, and in the meanwhile, power/current sharing of paralleled DAB modules is achieved. And according to Eq. (2), parameters (m_{xn} and L_{kxn}) of medium-frequency transformer in DAB will not affect current/power sharing of the paralleled DAB modules system.

Furthermore, we take module efficiency into account with different control methods. In our analysis, we assume the H-bridge and the DAB, which are connected with the same DC capacitor, as a module group. As shown in Figure 2, $\eta_{x1}, \eta_{x2}...\eta_{xn}$ are the module group efficiency, $P_{inx1}, P_{inx2}...P_{inxn}$ are the input power of module group, and $P_{ox1}, P_{ox2}...P_{oxn}$ are the output power of module group.

a) When the independent control for each stage is adopted, it means that DAB module output power $P_{ox1} = P_{ox2}...P_{oxn}$, thus,

$$P_{inx1} \cdot \eta_{x1} = P_{inx2} \cdot \eta_{x2} = ... = P_{inxn} \cdot \eta_{xn}. \tag{3}$$

The DC voltages of the H-bridge modules keep balance, which satisfy $\bar{u}_{dcx1} = \bar{u}_{dcx2} = ... = \bar{u}_{dcxn}$. And according to Eq. (3), we have:

$$d_{x1} \cdot \eta_{x1} = d_{x2} \cdot \eta_{x2} = ... = d_{xn} \cdot \eta_{xn} \tag{4}$$

From the analysis, we know that if different module groups have the same efficiency, there is no need to add DC voltage balancing and power/current sharing control method. Otherwise, different duty cycles are required for H-bridges to meet output current sharing of DAB modules.

b) When the proposed coordinated DC voltages control method is used, the controller of AC-Stage is responsible for the average DC voltage, and the controller of DC-Stage is in charge of the DC voltages balancing.

Since $d_{x1} = d_{x2} = ... = d_{xn}$, the input powers of different module groups are equal, $P_{inx1} = P_{inx2} = ...P_{inxn}$. Thus, we have:

$$P_{ox1}/\eta_{x1} = P_{ox2}/\eta_{x2} = ... = P_{oxn}/\eta_{xn}. \tag{5}$$

Furthermore, we can get:

$$I_{ox1}/\eta_{x1} = I_{ox2}/\eta_{x2} = ... = I_{oxn}/\eta_{xn}. \tag{6}$$

Eq. (6) indicates that if all the module groups work with the same efficiency, the output currents of DAB modules can be balanced naturally. Otherwise, the output current is proportional to its efficiency and reflects the imbalanced status of module group.

2.2. Interphase power characteristics

Interphase DC voltage balancing of cascaded H-bridge with star configuration is regulated by zero-sequence voltage injection or negative-sequence voltage/current injection [16, 17]. STATCOM function of SST, negative-sequence reactive power compensation, should be considered in the whole control. If negative-sequence voltage/current injection is used, the negative-sequence reactive current will be eliminated. As a result, only the zero-sequence voltage injection method can be used in independent control for each stage.

The three-phase voltage of power grid and currents of grid-connected cascaded SST with star configuration can be expressed by:

$$\begin{cases} e_a = e_p sin(\omega t), \\ e_b = e_p sin(\omega t - \frac{2}{3}\pi), \\ e_c = e_p sin(\omega t + \frac{2}{3}\pi), \end{cases} \tag{7}$$

$$\begin{cases} i_a = I_p sin(\omega t + \theta_p) + I_n sin(\omega t + \theta_n), \\ i_b = I_p sin(\omega t + \theta_p - \frac{2}{3}\pi) + I_n sin(\omega t + \theta_n + \frac{2}{3}\pi), \\ i_c = I_p sin(\omega t + \theta_p + \frac{2}{3}\pi) + I_n sin(\omega t + \theta_n - \frac{2}{3}\pi), \end{cases} \tag{8}$$

where e_p is the amplitude of positive-sequence voltage, I_p is the amplitude of positive-sequence current, I_n is the amplitude of negative-sequence current, θ_p is the corresponding phase angles of I_p, and θ_n is the corresponding phase angles of I_n.

As shown in Figure 3, the injection of zero-sequence voltage is equivalent to connection of a controlled voltage source u_z in the center of star configuration. Thus, phase current iA can be adjusted by the positive-sequence component u_p and the negative-sequence component u_n of the output voltage u_A of cluster A. u_z can be described by:

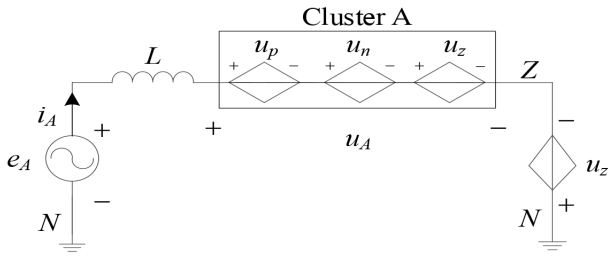

Figure 3. Equivalent model of single-phase with zero-sequence voltage injection.

$$u_z = V_z sin(\omega t + \varphi_z), \tag{9}$$

where V_z is the amplitude of the zero-sequence voltage, and φ_z is the corresponding phase angle.

The input active power of each cluster, P_x, can be calculated by the sum of the active power of power grid and controlled voltage source in each phase. To better understand the components of cluster power, the paper divides P_x into three parts, namely common active ΔP_x^{adj}, different active power ΔP_x^{sysj} caused by each phase of power grid, and adjustable active power ΔP_x^{adj} of interphase DC balancing method. The relationship of these input active power can be expressed by:

$$P_x = \bar{P} + \Delta P_x^{sys} + \Delta P_x^{adj} (x = A, B, C). \tag{10}$$

The $\bar{P}$, ΔP_x^{sys}, and ΔP_x^{adj} are derived as:

$$\bar{P} = \frac{1}{2} e_p I_p cos(\theta_p), \tag{11}$$

$$\begin{cases} \Delta P_A^{sys} = \frac{e+pI_n}{2} cos(\theta_n), \\ \Delta P_B^{sys} = \frac{e+pI_n}{2} cos(\theta_n - \frac{2}{3}\pi), \\ \Delta P_C^{sys} = \frac{e+pI_n}{2} cos(\theta_n + \frac{2}{3}\pi), \end{cases} \tag{12}$$

$$\begin{cases} \Delta P_A^{adj} = \frac{V_z}{2}[I + pcos(\varphi - \theta_p) + I_n cos(\varphi_z - \theta_n)], \\ \Delta P_B^{adj} = \frac{V_z}{2}[I + pcos(\varphi - \theta_p + \frac{2}{3}\pi) + I_n cos(\varphi_z - \theta_n) - \frac{2}{3}\pi)], \\ \Delta P_C^{adj} = \frac{V_z}{2}[I + pcos(\varphi - \theta_p - \frac{2}{3}\pi) + I_n cos(\varphi_z - \theta_n + \frac{2}{3}\pi)]. \end{cases} \tag{13}$$

Note that the latter two items in Eq. (10) do not affect the total input active power of AC-Stage (i.e. $\Delta P_A^{sys} + \Delta P_B^{sys} + \Delta P_C^{sys} = 0$, $\Delta P_A^{adj} + \Delta P_B^{adj} + \Delta P_C^{adj} = 0$) according to Eqs. (12) and (13). Therefore, ΔP_x^{adj} just adjusts the distribution of active power among clusters.

If the independent control for each stage is adopted, output active power of three clusters will be regulated to eventual consistency (i.e. $P_A \cdot \eta_A = P_B \cdot \eta_B A = P_C \cdot \eta_C$, where η_x is efficiency of cluster X) by active power adjustment ΔP_x^{adj}, which is produced by zero-sequence voltage injection u_z, and current sharing of paralleled DAB modules will be achieved simultaneously. However, interphase unbalanced handling capability of SST is limited by zero-sequence voltage and interphase power exchange is irrealizable as a result of current sharing control. Besides, paralleled DAB modules are likely to operate in hard-switching state with light load when SST just works in STATCOM mode.

If the proposed coordinated DC voltages control method is used, interphase unbalancing of cascaded H-bridges will lead into paralleled DAB modules of each phase and be solved by DC voltage balancing for paralleled DAB modules. Specifically, ΔP_x^{adj} is inexistent without zero-sequence voltage injection and ΔP_x^{sys} cannot be corrected in cascaded H-bridges. Meanwhile, the common DC bus of paralleled DAB modules can cancel out each ΔP_x^{sys}s among three phases. Thus, the negative-sequence voltage component of power grid and the negative-sequence reactive power compensation have no effect on SST. Furthermore, this control strategy aviods the additional voltage margin of cascaded H-bridges and fully utilizes idle power of the paralleled DAB modules, which is beneficial to satisfy soft-switching operation under STATCOM mode.

If the proposed coordinated DC voltages control method is used, interphase unbalancing of cascaded H-bridges will lead into paralleled DAB modules of each phase and be solved by DC voltage balancing for paralleled DAB modules. Specifically, ΔP_x^{adj} is inexistent without zero-sequence voltage injection and ΔP_x^{sysj} cannot be corrected in cascaded H-bridges. Meanwhile, the common DC bus of paralleled DAB modules can cancel out each ΔP_x^{sys} among three phases. Thus, the negative-sequence voltage component of power grid and the negative-sequence reactive power compensation have no effect on SST. Furthermore, this control strategy aviods the additional voltage margin of cascaded H-bridges and fully utilizes idle power of the paralleled DAB modules, which is beneficial to satisfy soft-switching operation under STATCOM mode.

In summary, the imbalance power is regulated in AC-Stage with the independent control or in DC-Stage with the coordinated DC voltages control. The proposed method has the same effect as the independent control for each stage under the ideal condition, which contains balanced power grid, coincident power module, and no negative-sequence reactive power compensation. Otherwise, the proposed method has been shown much better performance in interphase power balancing than the independent control for each stage due to interphase power exchange.

3. Coordinated DC voltages control strategy

Figure 4 shows the block diagram of a coordinated DC voltage control strategy developed for cascaded SST with star configuration. The positive- and negative-sequence current separate control strategy is utilized for AC-Stage as shown in Figure 4a. The negative-sequence current decoupling controller regulates the compensating negative-sequence reactive current depending on the system requirement. And the positive-sequence current

decoupling controller is used to control the average DC voltage of all the DC sides in AC-Stage and the positive-sequence reactive current. Different from the traditional control method, the imbalance power among different modules is not compensated in this stage. Therefore, the modulation voltages of clusters (u_a^*, u_b^*, u_c^*) is directly divided equally into n parts as module modulation voltage $(u_{ai}^*, u_{bi}^*, u_{ci}^*)$.

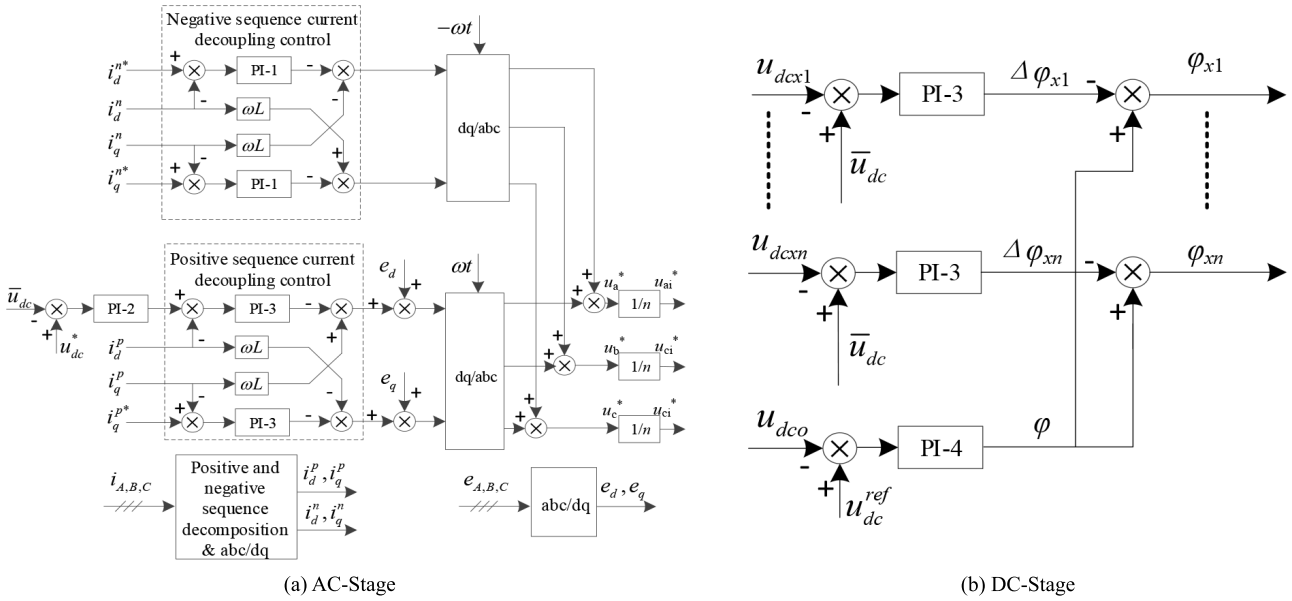

Figure 4. Coordinated DC voltages control strategy.

As depicted in Figure 4b, $3n$ phase-shift controller is applied to regulate power among DAB modules. The overall voltage loop regulates the output DC voltage udco of paralleled DAB modules, and generates the common phase-shifted angle φ. Meanwhile, the $3n$ voltage loops track the average DC voltage of AC-Stage to realize DC voltage balancing control, and form the phase-shifted angle corrections $(\Delta\varphi_{x1}, \Delta\varphi_{x2}, ..., \Delta\varphi_{xn})$. Eventually, the phase-shifted angles of DAB modules $(\varphi_{x1}, \varphi_{x2}, ...\varphi_{xn})$ are produced for DC-Stage.

Figure 5 is the comparison diagram between the proposed method and the traditional method. It can be seen that the proposed control method eliminates the interphase and inphase DC voltage balancing control, which greatly reduces the amount of calculation in the AC-stage. In the DC-Stage, the proposed method uses the voltage balancing control to realize the power sharing among DAB modules. Compared to the traditional current/power sharing control, the proposed system eliminates current sensors of DAB module and reduces the hardware cost without the control complexity increasement. For the control system, the number of PI controllers basically determines the time complexity of the control algorithm. Overall, the traditional method needs $6n+9$ PI regulators, but the proposed method only needs $3n+6$, which reduces the time complexity by half.

4. Simulation analysis

In order to verify the effectiveness and power characteristics of the coordinated DC voltages control strategy, an SST as shown in Figure 1 is implemented and analyzed using MATLAB/ Simulink. Besides, simulation-based comparisons in conditions of active power transmission and reactive power compensation are made between the traditional method and proposed method. The main simulation parameters are listed in Table 1.

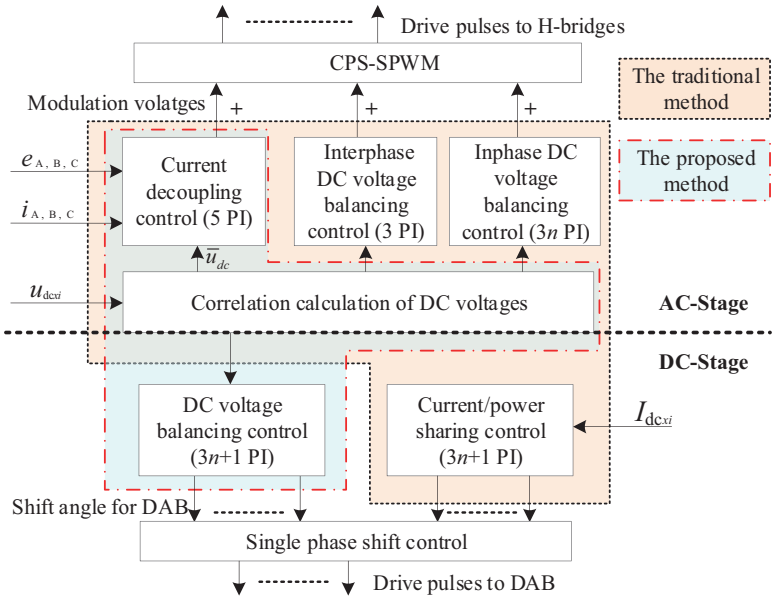

Figure 5. Equivalent model of single-phase with zero-sequence voltage injection.

Table 1. Main parameters of simulated cascaded SST.

Cascade number	2	Transformer ratio	Cluster A	60:63,60:58
Grid voltage	380 V		Cluster B	60:59,60:64
Grid frequency	50 Hz		Cluster C	60:60,60:61
Input inductance	3 mH	DAB leakage inductance	Cluster A	2.5, 2.3 mH
AC-Stage switching frequency	3.2 kHz		Cluster B	2.0, 2.4 mH
AC-Stage DC capacitance	6000 μF		Cluster C	3.3, 2.1 mH
AC-Stage DC voltage reference	250 V	Output DC capacitance		4000 μF
Equivalent loss of H-bridge	10 kΩ	Load resistor		2.3 Ω
DC-Stage switching frequency	1 kHz	Output DC voltage reference		250 V

4.1. Contrastive simulations of active power transmission

Figure 6 shows the steady-state simulation waveforms of the cascaded SST with balanced grid voltage and identical module efficiency. Comparing Figures 6a and 6b, it can be found that the control effects are almost identical for the two methods. Specifically, the three-phase grid-connected currents balancing, DC voltages equalization and currents sharing of DAB modules are well realized by the traditional and proposed methods, respectively. Besides, the differences of transformer ratio and leak inductance among all DAB modules have no effect on both methods.

Figure 7 shows the waveforms of SST using module groups with different efficiencies. Since imbalance factors of H-bridges and DAB modules can be equivalent to different paralleled resistors connected with DC capacitors, different resistors are linked to the secondary DC side of DAB (i.e. $R_{A1} = 1000, R_{A2} = 900, R_{B1} = 100, R_{B2} = 80, R_{C1} = 50, R_{C2} = 60$) so as to simulate different operating efficiencies of module groups. Note that, only average value waveforms of each cluster are shown in figures for a clear display.

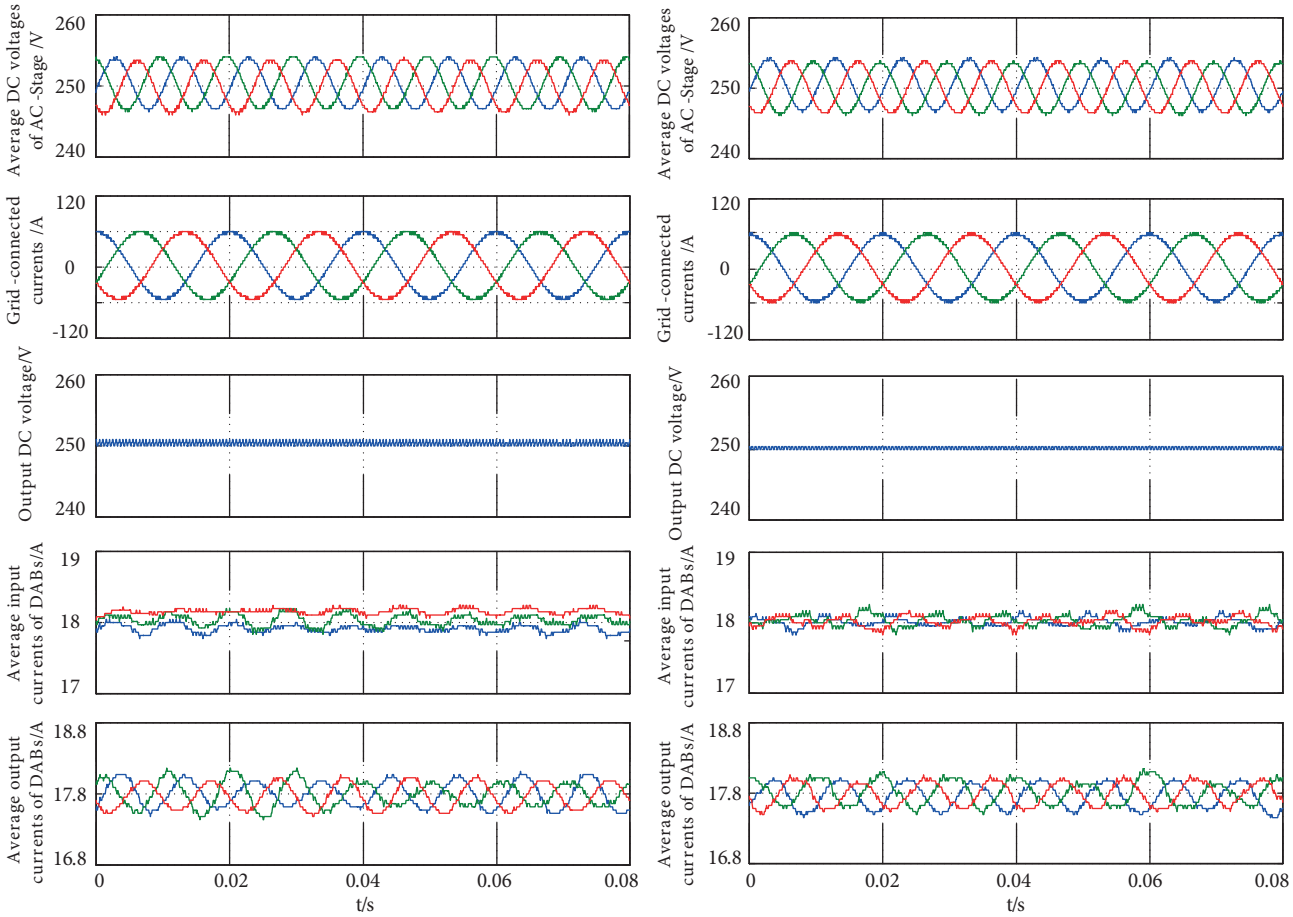

(a) The traditional control method

(b) The proposed control method

Figure 6. Steady-state waveforms of SST with ideal condition.

Figures 7a and 7b show the currents of DAB modules with the two methods, which can also indicate the power flow in module group. Note that, if the equivalent resistors simulating operating efficiencies are connected in different ways, the unbalanced currents of DAB modules will possibly be led with the proposed method.

Figure 7c shows the waveforms corresponding to the traditional control method. The output currents of DAB modules are balanced due to the current sharing control, but the input currents are unequal while the imbalance factor is introduced from DC-Stage into AC-Stage. The relationship among input power of three phase satisfies the previous analysis, $P_A \cdot \eta_A = P_B \cdot \eta_B = P_C \cdot \eta_C$. Therefore, zero-sequence voltage is injected for AC-Stage to regulate interphase power distribution, which results in balanced grid-connected currents, unbalanced modulation voltages of clusters and different DC voltage ripples in AC-Stage.

Figure 7 shows the simulation waveforms of SST with the proposed coordinated DC voltage control. Contrary to the results of the traditional method, the average input currents of DAB modules are equal as a result of average DC voltage regulation for AC-Stage, while the average output currents are unbalanced. Moreover, the DC voltage balance control for DC-Stage eliminates influence of power imbalance on AC-Stage. Then, the balanced modulation voltages and the same DC voltage ripples are achieved. The result shows that the proposed method has better DC voltage ripple performance with different module efficiencies.

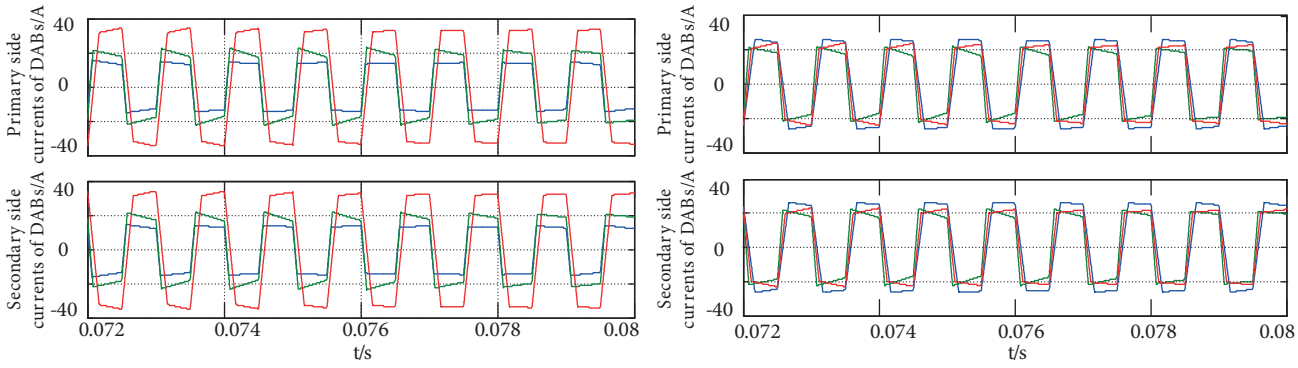

(a) The traditional control method

(b) DAB modules with proposed method

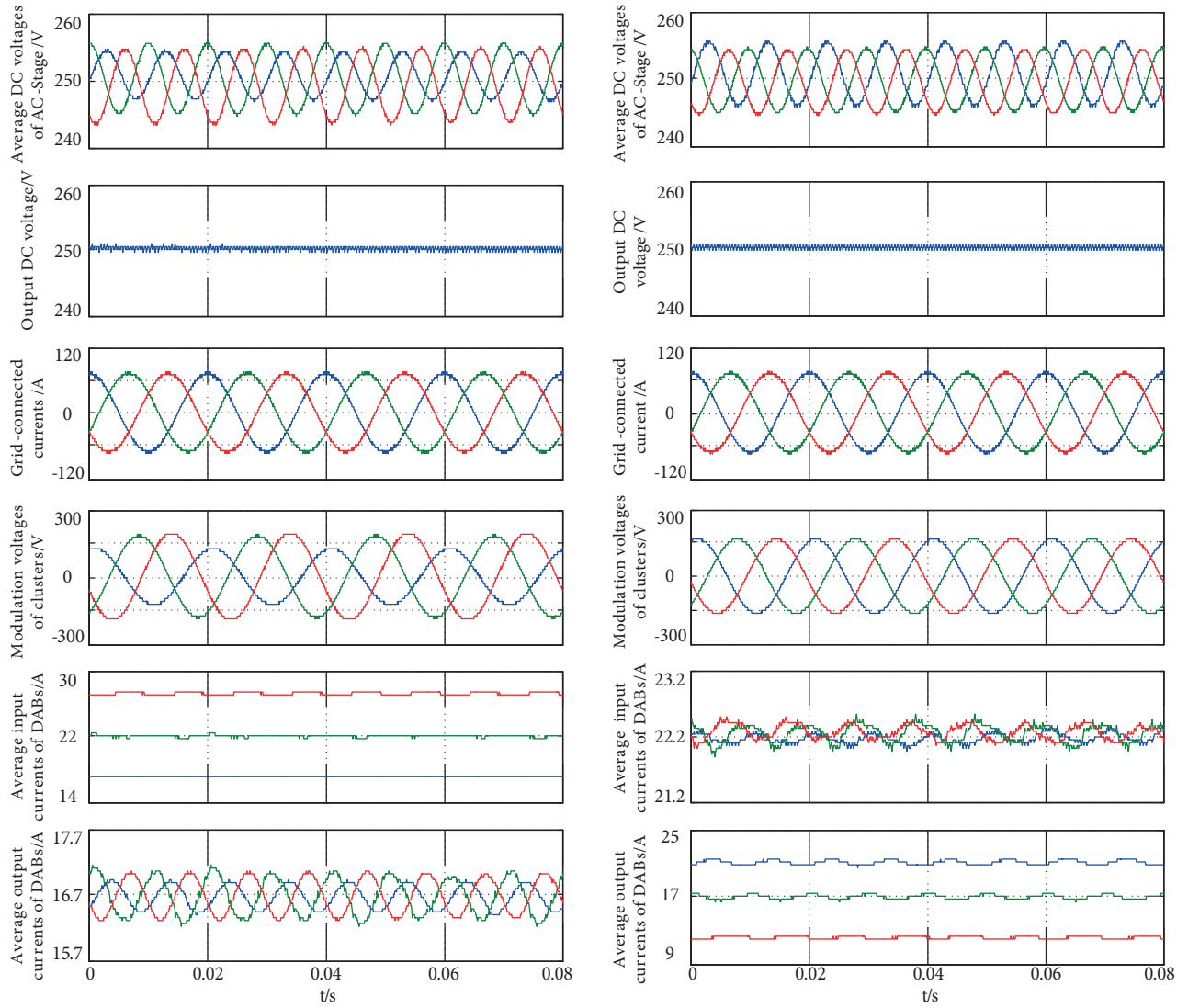

(c) Overall waveforms with traditional method

(d) Overall waveforms with proposed method

Figure 7. Waveforms of SST using module groups with different efficiencies.

4.2. Contrastive simulations of reactive power compensation

Figure 8a shows the simulation waveforms of reactive power compensation with traditional control method. The positive-sequence component of compensating currents reference is suddenly reduced from 20 A to 0 A, and the negative-sequence current rises from 5 A to 33.5 A at t = 0.05 s. As a result of the overmodulation, the DC voltages begin to diverge and the three-phase grid-connected currents also become distorted. The results show that the SST with traditional control method has limited interphase power regulation.

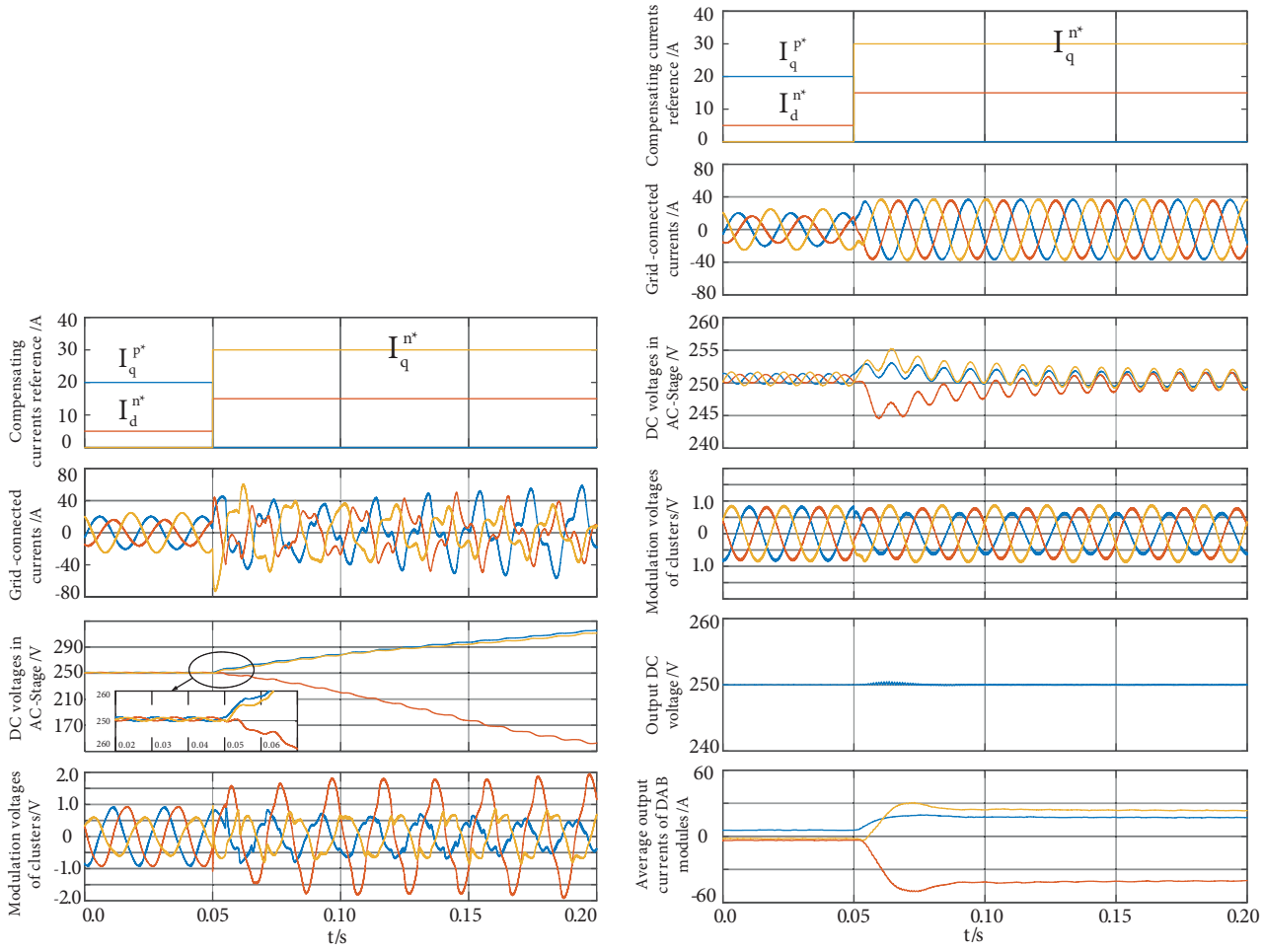

(a) The traditional control method

(b) The proposed control method

Figure 8. Waveforms of SST during sudden change of reactive currents.

Figure 8b shows the dynamic performance of SST using the coordinated DC voltages control method with a step of unbalance degree. First, the DC voltages in AC-Stage can maintain the reference value while the unbalance degree of negative-sequence current is 25%. Then, at t = 0.05 s, compensating negative-sequence currents reference increase and positive-sequence reactive currents reference reduces to zero. Meanwhile, DC voltages return to 250 V after the slight voltage fluctuation, and the average currents disparity among DAB modules increases owning to more interphase power exchange. The results show that arbitrary imbalance reactive compensation can be realized by the proposed method.

As expected from the simulation results, the proposed method achieves similar results compared to the

traditional method in the case of active power transmission, but the DC voltage ripple and current characteristics are different only when the unit efficiency is unequal. In the case of reactive power compensation, the traditional method does not have the ability of negative-sequence reactive power compensation, and the proposed method has arbitrary unbalanced reactive power compensation characteristic.

5. Experiment results

To better verify the effectiveness and feasibility of the coordinated voltages control method, an experimental SST platform as in Figure 9 is implemented. It adopts master–slave control mode, the master controller applies DSP-TMS320C28346 +FPGA-EP3C40 architecture, in which DSP is used for the main control algorithm and FPGA is for sending the control command and receiving information of power unit. All the CPLD slave controllers of power unit not only receive the control command from the master controller and then produce digital pulse signals, but also collect the information of power units and send them to the master controller. The AC side of three-phase clusters is connected by an adjustable transformer. The main parameters of the experimental SST are listed in Table 2. The SST platform consists of six power units, each of which contains an H-bridge module of the AC-stage and a DAB module of the DC-stage.

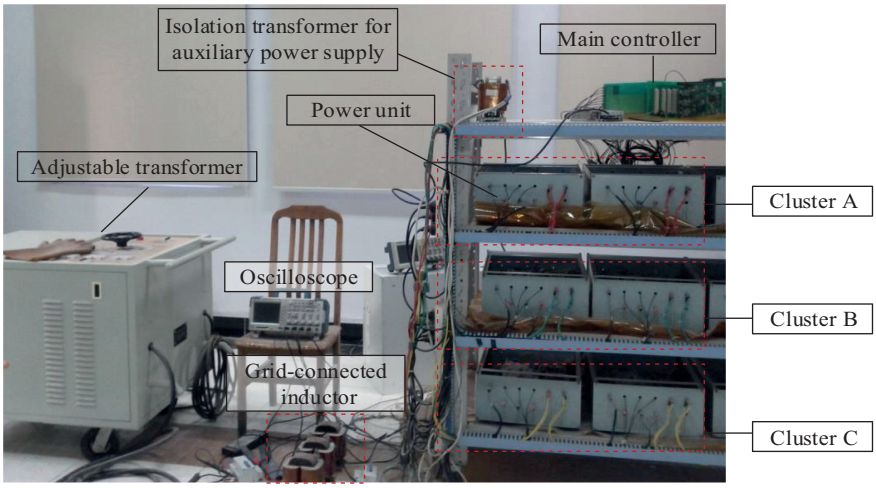

Figure 9. Experimental SST platform.

Table 2. Main parameters of experimental SST.

Cascaded number	2	DC-Stage switching frequency	1 kHz
Grid voltage	100 V	Transformer ratio	1:1
Grid frequency	50 Hz	DAB leakage inductance	1.8 mH
Input inductance	3 mH	Output DC capacitance	6667 μF
AC-Stage switching frequency	1.6 kHz	load resistor	3 Ω
AC-Stage DC capacitance	6667 μF	Output DC voltage reference	50 V
AC-Stage DC voltage reference	50 V	/	/

Figure 10 demonstrates the experimental waveforms of SST in steady-state with the proposed method, whose reactive current reference is set to zero. The line-to-line grid voltage, grid-connected currents, and DC output voltage are shown in Figure 10a. As can be seen, the ideal sinusoidal currents are produced, and the DC

output voltage maintains the reference value. Figure 10b shows the line-to-neutral grid voltage, grid-connected current and output voltage in phase A. There are five levels in cluster A with the PS-PWM modulation, and unity power factor is well realized. As shown in Figure 10c, the FFT results of cluster voltage indicate that the harmonic frequency is concentrated on 6.4 kHz, which is quadrupling switching frequency of AC-Stage. In Figures 10d and 10e, waveforms of one DAB with phase-shifting control are illustrated and currents of DAB modules are regulated to the balanced state. The simulation results show that the proposed method has a good control performance in steady-state and can meet the requirements of DC voltage balance and power balance for SST.

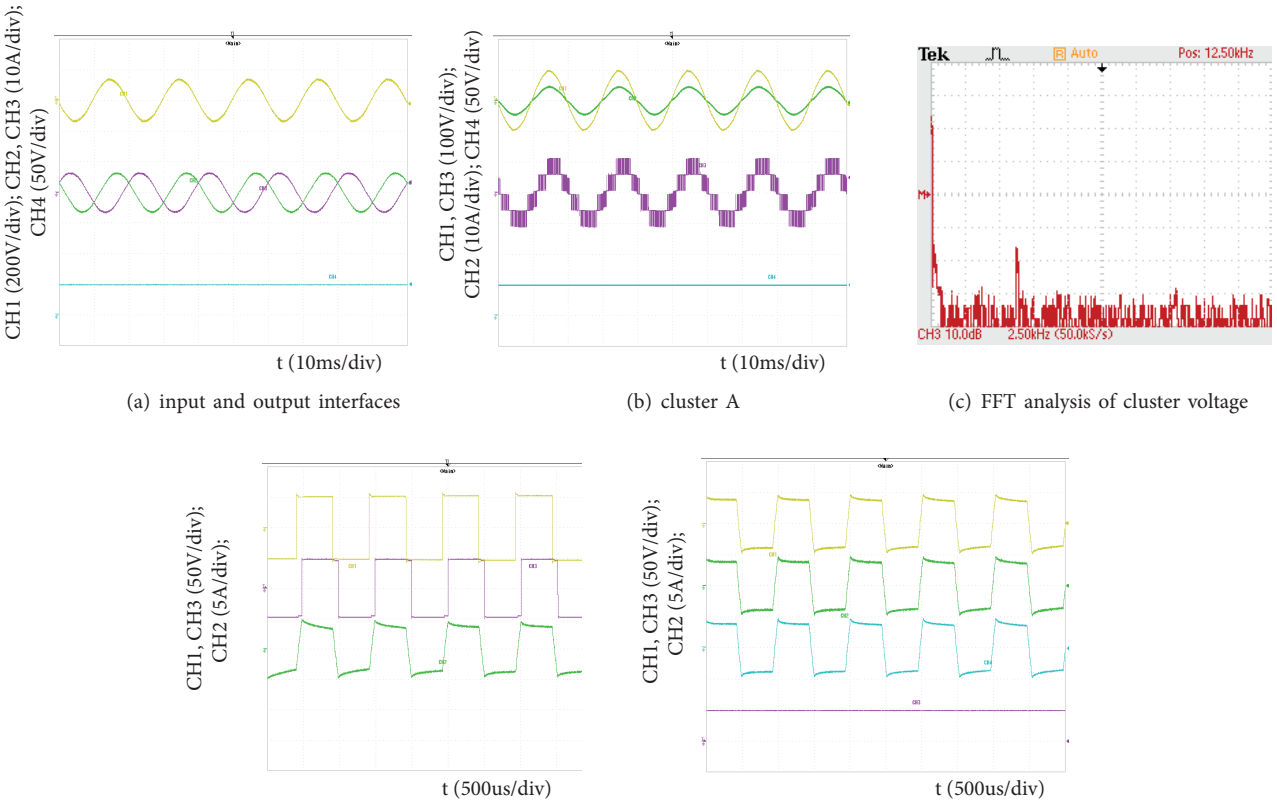

(a) input and output interfaces (b) cluster A (c) FFT analysis of cluster voltage

(d) DAB module in cluster A (e) DAB modules in different clusters

Figure 10. Experimental waveforms of cascaded SST in steady-state.

Figures 11a and 11b show the dynamic performance of SST during grid voltage changes. In this experiment, the DC output voltage of SST remains stable with the grid voltage dip and rise, and changes occur in grid-connected currents in order to maintain constant input power. So, the function of failure isolation between grid and load can be achieved by this proposed method in the SST platform.

6. Conclusion

In this paper, a coordinated DC voltage control method for cascaded SST with star configuration has been proposed. The new method makes full use of the common DC-Stage of the topological structure in order to realize power exchange among module groups. Compared with the traditional method, the proposed method can eliminate current sensors in DC-stage and reduce the calculation by half. Moreover, it not only enhances the stability of the control system with the consistency of DC voltage ripple, but also has the ability of arbitrary

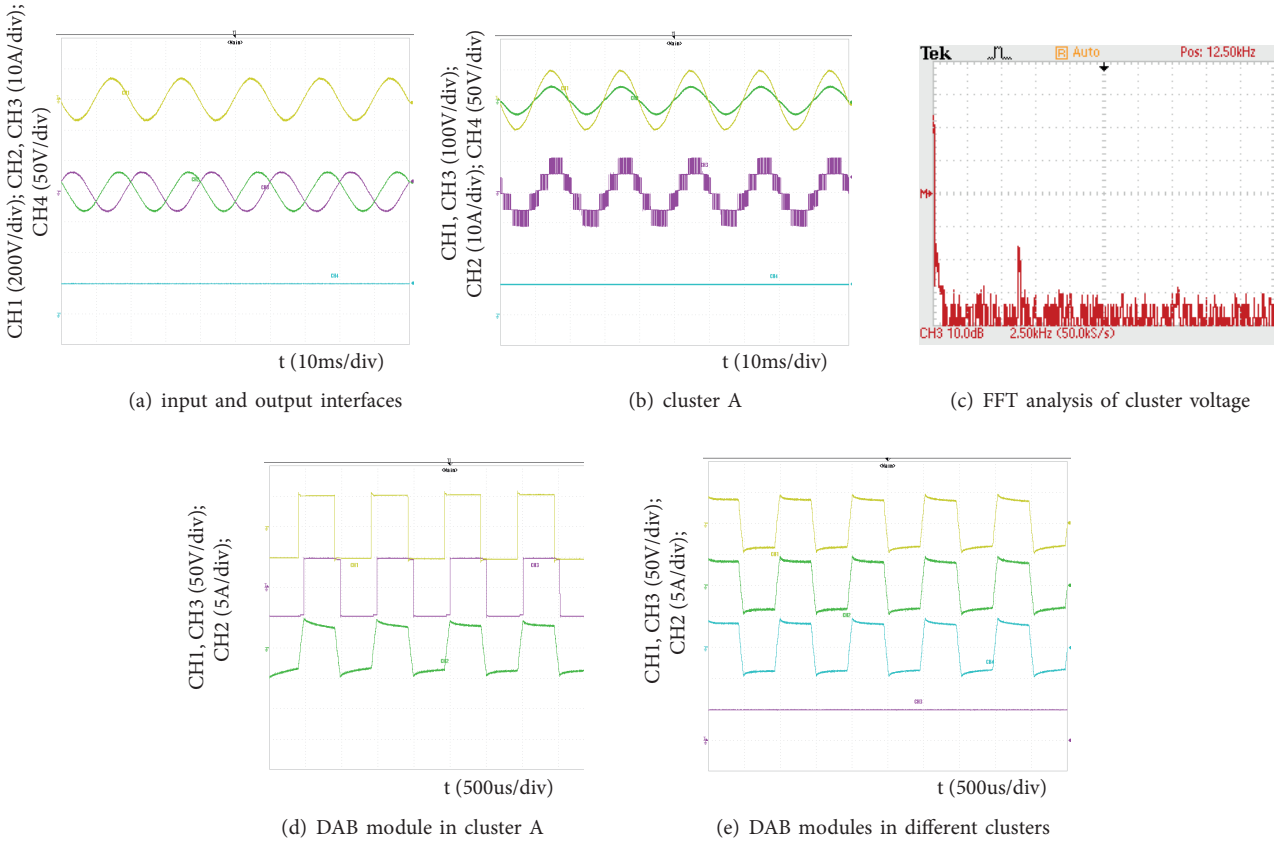

(a) input and output interfaces (b) cluster A (c) FFT analysis of cluster voltage

(d) DAB module in cluster A (e) DAB modules in different clusters

Figure 11. Experimental waveforms during grid voltage change.

unbalanced reactive power compensation. The inphase and interphase power characteristics in SST is analyzed, with which a coordinated DC voltage control strategy is achieved by regulating the average DC voltage and the balancing DC voltage in two stages respectively. The simulation and experiment results verify the effectiveness of the proposed method in both steady and dynamic states.

Acknowledgments

The work was supported by Natural Science Foundation of Jiangsu Province (NO. BK20170841) and Jiangsu Provincial Key Laboratory Foundation of Smart Grid Technology and Equipment.

References

[1] Costa LF, Carne GD, Buticchi G, Liserre M. The smart transformer: a solid-state transformer tailored to provide ancillary services to the distribution grid. IEEE Power Electron 2017; 4: 56-67.

[2] Huang AQ, Crow ML, Heydt GT, Zheng JP, Dale SJ. The future renewable electric energy delivery and management (FREEDM) system: the energy internet. P IEEE 2011, 99: 133-148.

[3] Xu S. Control and design of a high voltage solid state transformer and its Integration with renewable energy resources and microgrid system. PhD, North Carolina State University, North Carolina, USA, 2013.

[4] Dujic D, Kieferndorf F, Canales F, Drofenik U. Power electronic traction transformer technology. In: The 7th International Power Electronics and Motion Control Conference; 2–5 June 2012; Harbin, China. New York, NY, USA: IEEE. pp. 636-642.

[5] Lai JS, Maitra A, Mansoor A, Goodman F. Multilevel intelligent universal transformer for medium voltage applications. In: The 2005 Industry Applications Conference; 2–6 October 2005; Hong Kong, China. New York, NY, USA: IEEE. pp. 1893-1899.

[6] Falcones S, Mao X, Ayyanar R. Topology comparison for solid state transformer implementation. In: IEEE PES General Meeting; 25–29 July 2010; Providence, RI, USA. New York, NY, USA: IEEE. pp. 1-8.

[7] Song Q, Liu W. Control of a cascade STATCOM with star configuration under unbalanced conditions. IEEE T Power Electr 2009; 24: 45-58.

[8] Townsend CD, Summers TJ, Vodden J, Watson AJ, Betz RE, Clare JC. Optimization of switching losses and capacitor voltage ripple using model predictive control of a cascaded H-bridge multilevel StatCom. IEEE T Power Electr 2013; 28: 3077-3087.

[9] Liu J, Yang J, Zhang J, Zhao N and Zheng TQ. Voltage balance control based on dual active bridge DC/DC converters in a power electronic traction transformer. IEEE T Power Electr 2018; 33: 1696-1714.

[10] Jiang W, Huang L, Zhang L, Zhao H, Wang L, Chen W. Control of active power exchange with auxiliary power loop in a single-phase cascaded multilevel converter-based energy storage system. IEEE T Power Electr 2017; 32: 1518-1532.

[11] Wang C, Zhuang Y, Kong J, Tian C, Cheng H. Revised topology and control strategy of three-phase cascaded bridgeless rectifier. In: IEEE 43rd Industrial Electronics Society, Beijing, China, 2017; IEEE, pp. 1499-1504.

[12] Blahnik V, Kosan T, Peroutka Z, Talla J. Control of a single-phase cascaded H-bridge active rectifier under unbalanced load. IEEE T Power Electr 2018; 33: 5519-5527.

[13] Castillo R, Diong B, Biggers P. Single-phase hybrid cascaded H-bridge and diode-clamped multilevel inverter with capacitor voltage balancing. IET Power Electron 2018; 11: 700-707.

[14] Ye Z, Jiang L, Zhang Z, Yu D, Wang Z, Deng X, Fernando T. A novel DC-power control method for cascaded H-bridge multilevel inverter. IEEE T Ind Electron 2017; 64: 6874-6884.

[15] Lu D, Zhu J, Wang J, Yao J, Wang J, Hu H. A simple zero-sequence-voltage-based cluster voltage balancing control and the negative sequence current compensation region identification for star-connected cascaded H-bridge STATCOM. IEEE T Ind Electron 2018; 33:8376-8387.

[16] Yu Y, Konstantinou G, Townsend CD, Agelidis VG. Comparison of zero-sequence injection methods in cascaded H-bridge multilevel converters for large-scale photovoltaic integration. IET Renew Power Gen 2017; 11: 603-613.

[17] Vemuganti HP, Sreenivasarao D, Kumar DS. Zero-sequence voltage injected fault tolerant scheme for multiple open circuit faults in reduced switch count-based MLDCL inverter. IET Power Electron 2018; 11: 1351-1364.

[18] Lu D, Wang JF, Yao JH, Wang S, Zhu JX, Hu HB, Zhang L. Clustered voltage balancing mechanism and its control strategy for star-connected cascaded H-bridge STATCOM. IEEE T Ind Electron 2017; 64: 7623-7633.

[19] Iman-Eini H, Farhangi S, Schanen JL. A modular AC/DC rectifier based on cascaded H-bridge rectifier. In: The 13th International Power Electronics and Motion Control Conference; 1–3 September 2008; Poznan, Poland. New York, NY, USA: IEEE. pp. 173-180.

[20] Shi JJ, Gou W, Yuan H, Zhao T, Huang AQ. Research on voltage and power balance control for cascaded modular solid-state transformer. IEEE T Power Electr 2011; 26: 1154-1166.

[21] Zhao TF, Wang GY, Bhattacharya S, Huang AQ. Voltage and power balance control for a cascaded H-bridge converter-based solid-state transformer. IEEE T Power Electr 2013; 28: 1523-1532.

[22] Tian J, Mao CX, Wang D, Lu J, Liang X, Liu Y. Analysis and control of electronic power transformer with star-configuration under unbalanced conditions. IET Electr Power App 2015; 9: 358-369.

[23] Wang L, Zhang D, Wang Y, Wu B, Athab HS. Power and voltage balance control of a novel three-phase solid-state transformer using multilevel cascaded H-bridge Inverters for Microgrid Applications. IEEE T Power Electr 2016; 31: 3289-3301.

[24] She X, Huang AQ, Ni XJ. Current sensorless power balance strategy for DC/DC converters in a cascaded multilevel converter based solid state transformer. IEEE T Power Electr 2014; 29: 17-22.